ELSEVIER

Journal of Alloys and Compounds 271–273 (1998) 347–354

Journal of ALLOYS AND COMPOUNDS

Actinide nitrides and nitride–halides in high-temperature systems

T. Ogawa[a,*], F. Kobayashi[a], T. Sato[a], R.G. Haire[b]

[a] *Japan Atomic Energy Research Institute, Tokai-mura, Naka-gun, Ibaraki-ken, 319-11, Japan*
[b] *Oak Ridge National Laboratory, Oak Ridge, TN 37831-6375, USA*

Abstract

Knowledge of high-temperature actinide mononitrides systems has been extended in two fields. Systematics of the evaporation behavior of actinide mononitrides, including NpN and AmN, are discussed in view of recent experimental data. Secondly, for electrochemical data for the U–N–Cl system in molten salts let us consider equilibria in ternary systems containing halogens. The vaporization behavior of mononitrides together with other equilibrium relationships are described using a sublattice formalism, where the structural vacancy in the nitrogen sublattice is taken into account. © 1998 Elsevier Science S.A.

Keywords: UN; PuN; NpN; AmN; Vaporization; UNCl; UNF; Actinide nitride halide; Stability diagram; Thermodynamics

1. Introduction

In high-temperature systems, we have a high mobility of species and lowered kinetic barriers, which may either cause technical problems or offer new technological possibilities. Actinide mononitrides (AnN) are refractory materials, which gives them a potential for becoming a good nuclear fuel. However, they have relatively high volatilities at high temperatures in reactor accidents. Recently, knowledge on the high-temperature systems involving AnN has been extended in two fields. Vaporization measurements on NpN [1] and (Pu,(Am))N [2] have given insights into the systematics of the evaporation behavior of AnN. Electrochemical experiments on the U–N–Cl system in the LiCl–KCl eutectic melt [3] have let us estimate the equilibria in the ternary systems with halogens (X). The systematic understanding of the evaporation behavior of AnN may promote advanced fuel technologies. The equilibria in the An–N–X system have practical implications in the development of pyrochemical reprocessing of those fuels [4].

2. Evaporation behavior of mononitrides

Free energy of formation of AnN of light actinide elements from uranium to plutonium, and probably americium, is fairly constant. This is in contrast to pronounced atomic number dependence of the vaporization enthalpy of the actinide metals.

2.1. Thermochemical description

The data suggest that actinide mononitrides have narrow homogeneity ranges toward the hypostoichiometric side. The thermochemical properties of hypostoichiometric AnN_{1-x} can be modeled with a sublattice formalism [5,6]. Generally MN_{1-x} can be regarded as a series of regular solutions. Then, the free energy of formation is expressed by:

$$\Delta G_f^\circ = Y_N\,\Delta G_f^\circ(\mathrm{MN}) + Y_V\,\Delta G_f^\circ(\mathrm{MV}) + Y_N Y_V L + RT(Y_N \ln Y_N + Y_V \ln Y_V), \quad (1)$$

where $\Delta G_f^\circ(\mathrm{MN})$ is the free energy of formation of stoichiometric MN, $\Delta G_f^\circ(\mathrm{MV})$ is that of a hypothetical species, in which all nitrogen atoms in MN are replaced by vacancies, L is a constant called the interaction parameter, Y_N is the atomic ratio N/Pu, and $Y_V = 1 - Y_N$. Since actinide mononitrides exhibit NaCl-type structures, MV is taken to be the pure actinide metal having the fcc structure. $\Delta G_f^\circ(\mathrm{MV})$ would have a value of the order of the free energy of allotropic transformation, ΔG_t. The ΔG_t for the transformation of bcc-U to the hypothetical fcc-U has been estimated by modeling the U–Pu phase diagram [7]. The M–MN liquid phase is described in the same manner as the solid MN_{1-x}.

The metal activity and nitrogen partial pressure are given by:

*Corresponding author: Tel.: 81 29 2825430; fax: 81 29 2826097; e-mail: ogawa@sun2sarl.tokai.jaeri.go.jp

0925-8388/98/$19.00
PII: S0925-8388(98)00086-3

$$RT \ln a(\mathrm{M}) = \Delta G_f^\circ(\mathrm{MV}) + Y_N^2 L + RT \ln Y_V, \quad (2)$$

$$(1/2)\, RT \ln p(\mathrm{N_2}) = \Delta G_f^\circ(\mathrm{MN}) - \Delta G_f^\circ(\mathrm{MV}) + (Y_V - Y_N)L + RT(\ln Y_N - \ln Y_V). \quad (3)$$

The equilibrium constant, $K_p = p(\mathrm{M})[p(\mathrm{N_2})]^{(1/2)}$, is then written:

$$RT \ln K_p = -\Delta G_f^\circ(\mathrm{M(g)}) + \Delta G_f^\circ(\mathrm{MN}) + (1 - Y_N)^2 L + RT \ln Y_N, \quad (4)$$

where $\Delta G_f^\circ(\mathrm{M(g)})$ is the free energy of formation of the metal monatomic gas. When the deviation from stoichiometry is small, contributions of the third and fourth terms are minor relative to those of the first and second terms in Eq. (4). Therefore, the partial pressures at the congruent vaporizing composition can be estimated from $\Delta G_f^\circ(\mathrm{MN})$ and $\Delta G_f^\circ(\mathrm{M(g)})$ fairly accurately, without detailed knowledge of the equilibrium involving the nitride phase. The congruent vaporization is realized when:

$$p(\mathrm{M})/p(\mathrm{N_2}) = 2\sqrt{M(\mathrm{M})/M(\mathrm{N_2})}, \quad (5)$$

where M is the molecular mass. On the other hand, the equilibrium compositions such as the congruent vaporizing composition and the phase boundaries cannot be calculated without the parameter L. Conversely, the parameter L cannot be fixed without detailed knowledge of the phase equilibria or the activity–composition relationship. Given such detailed data, the above model can be extended to the subregular solutions by the Redlich–Kister-type formulation [8].

The gaseous species considered are M(g) and N_2(g). There are certainly other possible gas species, such as MN(g) and M_2(g), but their contributions to the general equilibria can be neglected [9]. In the experimental measurements, particularly on UN and NpN, complications arise from the presence of MO(g). The present analysis does not consider the ternary system containing oxygen, but concentrates on the ideal cases involving nitrogen as the only nonmetal element. The equilibrium calculations have been made with a code ''Chemsage'' [10]. (Below, the specific values of partial pressures are given by a nondimensional expression: $p^* = p(\mathrm{Pa})/1.01325 \times 10^5(\mathrm{Pa})$).

2.2. Uranium mononitride

Uranium mononitride is thermodynamically stable up to its melting point. However, a liquid uranium phase segregates out at higher temperatures due to the preferential vaporization of nitrogen. The contribution of UN(g) is negligibly small, compared with N_2(g) and U(g) in the overall vaporization of uranium mononitride. Thermodynamic properties of uranium mononitride have been measured extensively, and assessed by several authors [7,10–13]. Nevertheless, there still remains a difficulty: there is an inherent disagreement among the assessed data for the Gibbs free energy of formation, (ΔG_f°) of UN(s), the decomposition pressures of UN(s) (Fig. 1) and the solubility limit of nitrogen in liquid uranium, particularly at temperatures below 2800 K [5].

In taking compromise between the assessed enthalpy of formation (ΔH_f°) of UN(s) and the decomposition pressures in the literature, Oetting and Leitnaker [13] had assumed an activity of U, a(U), of 0.5 in nitrogen-saturated liquid uranium at temperatures around 1600 K. This assumption is questionable for the following reasons:

1. Solubility of nitrogen in liquid uranium at 1600 K is very small, ~0.1 at% [11,14,15].
2. One can estimate p(U) at higher temperatures ($T > 2800$ K), where the nitrogen solubility in liquid uranium exceeds 24 at% [14,15]. The decomposition pressure $p(\mathrm{N_2})$ has been measured by Olson and Mulford [16], and the equilibrium constant for the reaction, UN(s) = U(g) + (1/2)N_2(g), by Alexander et al. [17]. The temperature ranges of these two independent sets of measurements overlap at 2800–2900 K. If the enthalpy of vaporization of uranium is taken to be 531 kJ mol^{-1} [18], one obtains a(U) = 0.6 at 2900 K, which increases to 0.7 at 2800 K.
3. Nitrogen in transition metals does not produce a large stabilization. It has been assessed that, at 2000 K, a(Zr) is 0.75 in α-Zr with 24 at% nitrogen, and is 0.94 in β-Zr with 6 at% nitrogen, both referring to pure β-Zr [19]. This assessment is consistent with $\Delta G_f^\circ(\mathrm{ZrN(s)})$ [20], the decomposition pressure [21,22] and the phase diagram [23].

Thus, it is considered more reasonable to assume that

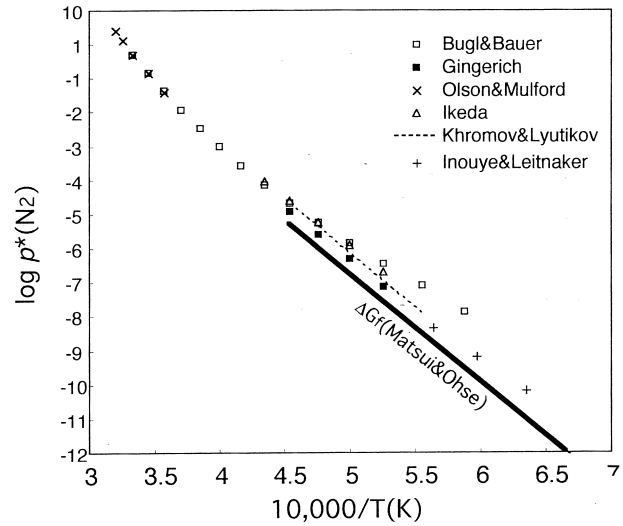

Fig. 1. Experimental decomposition pressures of UN [15,16,24–27] compared with those calculated from ΔG_f°(UN(s)) by Matsui and Ohse [10], assuming a(U) = 1.

a(U) is closer to unity at temperatures around 1600 K. If a(U) is closer to unity, and the assessed ΔG_f°(UN) values in the compilations [10,11,13] are correct, we cannot but question the measured UN decomposition pressures [15,16,24–27] at lower temperatures. An alternative approach is to adjust ΔG_f°(UN(s)) by approximately, $-RT \ln 0.5$ ($=\sim 9$ kJ mol^{-1} at 1600 K), to reproduce the measured decomposition pressures. This discrepancy appears a little too large in view of the estimated errors in ΔH_f°(UN(s)) which is about ± 4 kJ mol^{-1} [10,13]. However, the enthalpy of vaporization of uranium, which has been used in estimating the third-law enthalpy of formation of UN(s) from the vaporization data, is estimated to have error limits of -4 and $+8$ kJ mol^{-1} [18].

In reproducing the observed high-temperature behavior of UN and (U, Pu)N nuclear fuels at temperatures 1400–2500 K [7], the ΔG_f°(UN(s)) adjusted to the decomposition pressure data by Tagawa [28] has been successfully applied:

$$\Delta G_f^\circ(\mathrm{UN(s)})(\mathrm{J\ mol^{-1}}) = -306\,089 + 94.278T. \quad (6)$$

The other pertinent parameters are given in Table 1. Predicted $p(N_2)$ and a(U) in the U(l)+UN two-phase region are shown in Fig. 2. This figure may be referenced in discussing the vaporization behavior of the other actinide mononitrides.

The above equation for ΔG_f°(UN(s)) is less negative than that obtained by fitting thermodynamic functions assessed by Matsui and Ohse [10]:

$$\Delta G_f^\circ(\mathrm{UN(s)})(\mathrm{J\ mol^{-1}}) = (-303\,984 \pm 574) + (87.65 \pm 0.27)T \quad (1500 - 3000\ \mathrm{K}). \quad (7)$$

It is interesting to see that the difference between these two equations, when divided by T(K), is nearly constant ($-R \ln 0.5$), although the nitrogen solubility in liquid uranium increases by a factor of ~ 200 with increasing temperature from 1500 to 2500 K.

2.3. Plutonium mononitride

We find only six sets of data [29–34] reported for the vaporization of PuN(s). The consistency among the data sets has been studied with the model described above. Parameters for PuN are given in Table 2 [7]. The smaller enthalpy of formation of Pu(g), compared with that of U(g), allows PuN(s) to vaporize congruently. The prediction is consistent with p(Pu) over PuN(s) by Kent and Leary [29], and by Suzuki et al. [31]; p(Pu) over Pu(l)+PuN(s) by Kent and Leary [29]; the congruent vaporization composition by Kent and Leary [29] and by Alexander et al. [30]; the decomposition pressures, $p(N_2)$, of PuN(s) by Olson and Mulford [32] and by Alexander et al. [34]. Fig. 3 compares the calculated decomposition pressures with the experimental data. Although the data by Olson and Mulford [32] were for temperatures above 2563 K, both the data by Alexander et al. [34] and the present model

Table 1
Parameters for modeling of U–UN system for $T = 2000$–3000 K

Species	ΔG_f° (J mol^{-1})
UN(s)	$-306\,089 + 94.278T$
UV(s)	$-13\,279 + 10.631T$
UN(l)	$-251\,208 + 76.71T$
UV(l)	0
Pair	L (J mol^{-1})
UV(s)–UN(s)	$10\,000 + 20T$
UV(l)–UN(l)*	L_1: $1205\,500 - 7213.5T + 922.26T \ln T - 0.18691T^2$
	L_2: $-181\,790 + 67.33T$

UV(l)–UN(l) is assumed regular up to 2700 K with only one parameter L_1. Above 2700 K it is assumed subregular with two parameters L_1 and L_2.

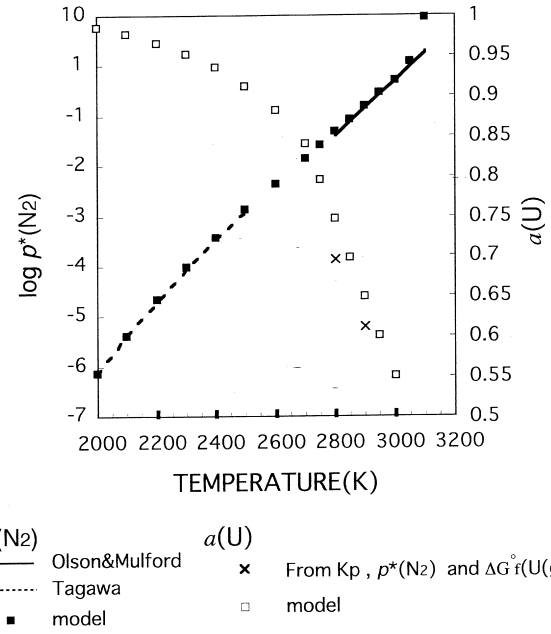

Fig. 2. Modeling prediction of $p(N_2)$ and a(U) in the U(l)+UN(s) two-phase region. Experimental decomposition pressures are by Olson and Mulford [16] and those fitted by Tagawa [11]. Experimental a(U) is estimated by combining the decomposition pressure by Olson and Mulford and the equilibrium constant K_p by Alexander et al. [17]. ($p^* = p$(MPa)/10.1325).

Table 2
Parameters for modeling Pu–PuN system for $T = 2000$–2400 K

Species	ΔG_f° (J mol^{-1})
PuN(s)	$-296\,691 + 84.366T$
PuV(s)	$-4770 + 5.69T$
PuN(l)	$-244\,091 + 66.796T$
PuV(l)	0
Pair	L (J mol^{-1})
PuV(s)–PuN(s)	$-60\,800 + 46.4T$
PuV(l)–PuN(l)	$-84\,000 + 45T$

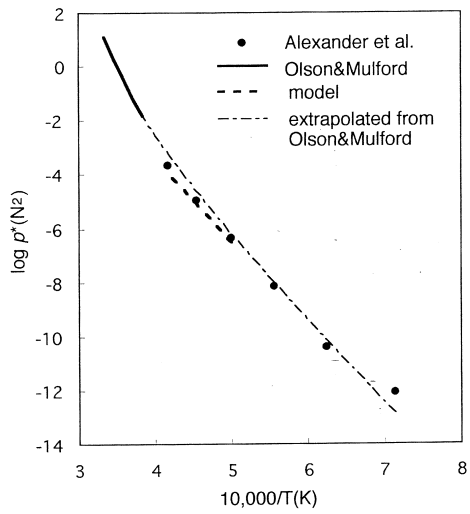

Fig. 3. Decompsition pressures of PuN(s): Comparison of the experimental data [32,34] versus model calculations.

prediction are consistent with the extrapolation of Olson and Mulford's equation for $p(N_2)$ to lower temperatures,

$$\log_{10} p^*(N_2) = 8.193 - 29.54 \times 10^3/T + 11.28 \times 10^{-18} T^5. \quad (8)$$

A liquid Pu phase should not be observed below the decomposition pressures, due to rapid vaporization of Pu. Thus, except for high $p^*(N_2)$, exceeding ~0.03 (0.003 MPa) [32], the experimental decomposition pressure in Fig. 2 should be regarded as the minimum pressure needed to retain the PuN(s) phase for observation.

The p(Pu) data by Kent and Leary have been corrected for the thermodynamic data for a Au standard in the Knudsen-cell effusion mass-spectrometry measurements, as suggested by Oetting et al. [18]. The correction improved the agreement between the data by Kent and Leary and those by Suzuki et al. The p(Pu) over PuN(s) reported by Marcon and Poitreau [33] is incongruous with the other data sets: their data suggest that nitrogen-saturated Pu(l) segregates from PuN(s) at temperatures higher than 1930 K.

The free energy of formation, ΔG_f°, of stoichiometric PuN(s) adopted in the model calculation is more negative by 20 kJ mol^{-1} than those given by the preceding assessments [10,12].

Alexander et al. [30] have measured the equilibrium constant, K_p, for the reaction, $PuN(s) = Pu(g) + N_2(g)$, using a vacuum thermobalance-effusion technique. The p(Pu) values over PuN(s) at the congruent vaporization, which is estimated from their K_p, is slightly higher by a factor of 1.3–1.5 than those by Kent and Leary [29] and by Suzuki et al. [31]. The ΔG_f°(PuN(s)) from the experimental K_p and ΔG_f°(Pu(g)) [18] becomes less negative by ~5 kJ mol^{-1} than that given in Table 2. The scatter in the measured K_p, however, is not small and corresponds to estimated errors of ±8 kJ mol^{-1} in ΔG_f°(PuN(s)). The error limits of ΔG_f°(Pu(g)) would not be smaller than ±4 kJ mol^{-1}.

With the parameters in Table 2, the phase boundaries of the Pu–N binary system can be calculated. The only experimental point is by Alexander et al. [35]: the lower homogeneity range of PuN at 2350 K was found at $p^*(N_2) = 1.0 \times 10^{-4}$ and N/Pu = 0.954. The present model gives $p^*(N_2) = 6.6 \times 10^{-5}$ and N/Pu = 0.946. However, the model gives a significantly wide homogeneity range at lower temperatures: the lower phase boundary of the PuN phase lies at N/Pu = 0.89 at 2000 K. Only with such a wide homogeneity range, could the experimental data summarized above be satisfactorily reproduced within the regular-solution type sublattice formalism. For further optimization, or the extension of the model to the subregular type solutions, experimental data for the phase boundaries are needed. Thus, the applicability of the parameters in Table 2 outside the range of 2000–2400 K should be questioned.

2.4. Neptunium mononitrides

There are only two sets of data on the vaporization behavior of NpN: Olson and Mulford [36] obtained the decomposition pressure at temperatures 2483–3103 K; Nakajima et al. [1] measured p(Np) over NpN by Knudsen-cell effusion mass spectrometry at temperatures 1690–2030 K. The data by Olson and Mulford suggest that NpN is similar in thermodynamic stability to UN and PuN. The expected large solubility of nitrogen in liquid Np at high temperatures prevents deriving ΔG_f°(NpN) from their data alone. Nakajima et al. have found that p(Np) over NpN is close to that over pure Np by Ackermann and Raugh [37], both in magnitude and temperature dependence. Actually p(Np) by Nakajima et al. was even a little higher than that of pure Np. Hence, one may at least say that a(Np) is close to unity over Np(l) + NpN at 1690–2030 K. The temperature ranges between the data of Olson and Mulford and those by Nakajima et al. differ so widely that it is difficult to combine them by simple extrapolations. In this regard, Fig. 2 for the U–N system should be consulted.

An interesting behavior recurred in measuring p(Np) over NpN by Knudsen-cell effusion mass spectrometry [38]: p(Np) was significantly smaller in the first heating run versus succeeding runs on the same sample. p(Np) over NpN was reported by Nakajima et al. [1] only after the first heating run. The two curves merged at ~1950 K. This behavior can be explained if ΔG_f°(NpN) is approximated by ΔG_f°(PuN) given in Table 2. Fig. 4 shows a prediction with ΔG_f°(Np(g)) in Ref. [18] and ΔG_f°(NpN) = ΔG_f°(PuN). In view of this prediction, NpN vaporizes congruently to ~1950 K in the first heating run, then segregates a nitrogen-saturated liquid phase at higher temperatures. The liquid phase may have been preserved

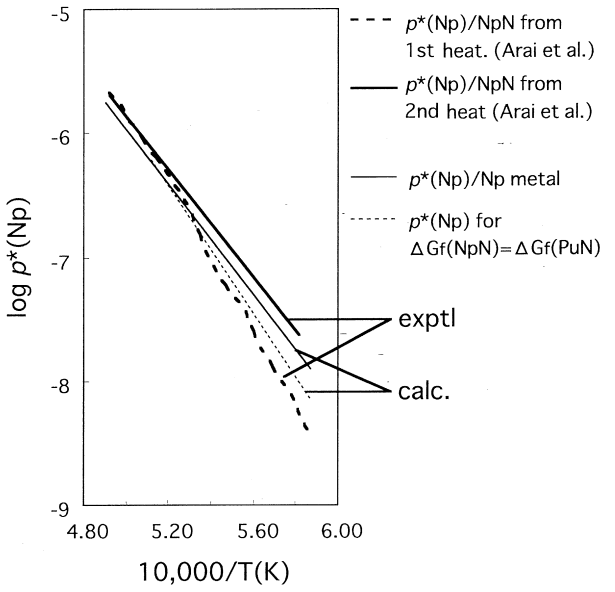

Fig. 4. Predicted transition from congruent vaporization (thin dotted line) to decomposition (thin solid line) of NpN(s) assuming $\Delta G_f^\circ(\mathrm{NpN(s)}) = \Delta G_f^\circ(\mathrm{PuN(s)})$. Thick dashed line is the experimental $p(\mathrm{Np})$ in the first heating run on a NpN sample by a Knudsen-cell effusion mass spectrometry; thick solid line is from subsequent runs [38].

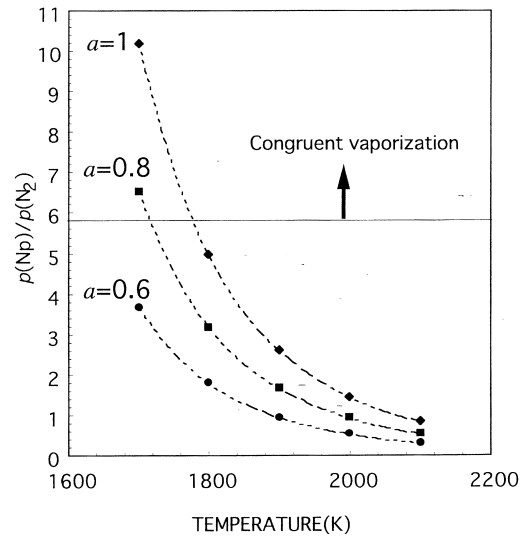

Fig. 5. Calculated pressure ratio $p(\mathrm{Np})/p(\mathrm{N_2})$ in the Np(l)+NpN(s) two-phase region as a function of assumed $a(\mathrm{Np})$. When $p(\mathrm{Np})/p(\mathrm{N_2})$ over Np(l)+NpN(s) exceeds 5.82 at a given temperature, congruent vaporization occurs within the homogeneity range of NpN(s).

during the succeeding cooling run due to relatively low vapor pressure of Np.

It is also probable that this type of behavior is related to some impurities in the sample, which may have had stronger effects in the first heating run than in the succeeding runs. Then one would have to discard the data from the first heating run. Actually, the reproducibility of the data of the first heating runs on NpN samples was poor, while that of the data from the succeeding runs was excellent. The second-law enthalpy of formation based on the experimental curve for the first heating run in Fig. 4 (thick dashed line) is too large compared with ΔH_f° for UN(s) and PuN(s), although $\Delta G_f^\circ(\mathrm{NpN(s)})$ calculated on the same curve becomes plausible (-145 kJ mol^{-1} compared with -143 kJ mol^{-1} for PuN at 1820 K).

However, it should be noted that, if $\Delta G_f^\circ(\mathrm{NpN})$ is less negative and closer to $\Delta G_f^\circ(\mathrm{UN})$ given in Table 1, the departure from the congruent vaporization would occur at 1700–1800 K, unless there is a substantial solubility of nitrogen into liquid metal at these temperatures to make $a(\mathrm{Np})$ significantly lower than unity ($a(\mathrm{Np}) \leq 0.8$). Fig. 5 gives $p(\mathrm{Np})/p(\mathrm{N_2})$ over Np(l)+NpN(s) as a function of $a(\mathrm{Np})$ in the two-phase region. The $\Delta G_f^\circ(\mathrm{NpN})$ is assumed to be equal to $\Delta G_f^\circ(\mathrm{UN})$, and the third and fourth terms in Eq. (4) are neglected. When $p(\mathrm{Np})/p(\mathrm{N_2})$ is smaller than 5.82 in the two-phase region, one does not see the congruent vaporization within the homogeneity range of NpN(s). Thus, it is considered likely that the transition from congruent vaporization to decomposition occurs at a temperature between 1700–2000 K for neptunium mononitride.

2.5. Americium mononitride

There is only one set of data on the vaporization of americium mononitride, which has been obtained by a Knudsen-cell effusion mass spectrometer for the reactor-grade plutonium mononitride sample [2]. The plutonium contained about 1.3 at% of ^{241}Am as a daughter product of ^{241}Pu. A significantly large mass-241 signal was noted in the initial heating run, while the mass-239 signal was anomalously low. Eventually, the mass-241 signal subsided, and the mass-239 signal then reached a level that agrees with previous measurements by Kent and Leary for PuN of a weapons-grade plutonium [29].

This anomalous vaporization behavior has been explained by assuming that $\Delta G_f^\circ(\mathrm{AmN(s)}) \cong \Delta G_f^\circ(\mathrm{PuN(s)})$. It is certainly due to significantly smaller $\Delta H_f^\circ(\mathrm{Am(g)})$ (284 kJ mol^{-1} [18]) as compared with other actinide metals. A detailed analysis of the observed behavior has been described [2]. The second-law enthalpy of formation of AmN(s) from Am(g) and N_2(g) has been estimated from the observed partial pressures of Pu(g) and Am(g) after the mass-241 signal subsided: -294 kJ mol^{-1}, which is very similar to those of UN(s) and PuN(s). However, this derivation assumes that the surface concentration of americium in the plutonium nitride sample is nearly constant after the initial ^{241}Am burst subsided. We plan to supplement this estimate by measurements using pure AmN prepared via metallic americium.

The observation made with the reactor-grade PuN sample is a good example of the complex behavior of mixed actinide mononitrides. Although $\Delta G_f^\circ(\mathrm{MN(s)})$ is considered similar to each other, $\Delta G_f^\circ(\mathrm{M(g)})$ depends strongly on the element. With decreasing vaporization enthalpy of the element, the congruent vaporization com-

position of a mononitride tends to shift to higher nitrogen content for a given temperature. These facts cause appreciably different partial pressures of metal vapors immediately above the surface of mixed nitrides. The actual vaporization process is also controled by the solid-state diffusion, which may result in a steep concentration gradient below the solid surface. These factors may give a notable time dependence on the observed partial pressures over the mixed nitrides during the initial part of study. Thus, it would be difficult to derive an accurate activity–composition relationship from the vaporization measurements of mixed nitrides. The composition of the metal sublattice near the surface may be significantly different from the bulk composition. An interesting observation on the surface depletion of plutonium in (U,Pu)N has been made by Bradbury and Matzke [39].

3. Actinide–nitrogen–halogen system

Ternary systems with one more nonmetal elements have been studied largely because of their implication in the nitride fabrication processes: there is a substantial database on An–N–C and An–N–O systems [12,40–42]. The behavior of ternary systems with halogens (An–N–X) is less defined. The ternary compounds, UNCl, UNBr and UNI, have been prepared and their structures determined by Juza and Meyer [43]. The ternary compound UNF has been identified by Yoshihara et al. [44].

3.1. U–N–Cl

Kobayashi et al. found that solid UNCl was formed during anodic decomposition of UN pellets in LiCl–KCl eutectic melt [3]. UNCl showed a very small solubility ($\leq 7\times10^{-3}$ wt% U) in the eutectic melt. The apparent e.m.f. of the cell, UN(s)|UNCl(saturation), LiCl–KCl|LiCl–KCl, Ag^{+} ($x=0.1$)|Ag, was measured. It was not clear in which form UNCl was dissolved in the salts. However, the measured e.m.f. agreed with the anodic potential, where UN pellets started to decompose in fused salts of LiCl–KCl–UCl_3.

The e.m.f. at the saturation of UNCl in LiCl–KCl was -1.03 V at 773 K, which is translated to $E=-2.08$ V against Cl_2/Cl^-, using the literature value of ΔG_f°(AgCl) [45]. It is assumed that the activity coefficient of AgCl in the salt was approximately unity. A small difference between ΔG_f°(AgCl(s)) and ΔG_f°(AgCl(l)) is neglected, the stability diagram at 773 K is shown in Fig. 6. The previous data [46] of the anodic decomposition of UN pellets are also shown for comparison. The stability diagram provides a basis for understanding the behavior of the other An–N–X systems.

3.2. U–N–F

The equilibria in the U–N–F ternary system have been studied by Tagawa [47]. The reaction product was UF_3 for $3UF_4+UN$ mixtures; it was UNF for UF_4+3UN mixtures in a nitrogen atmosphere. The equilibrium $p(N_2)$ over $UN+UF_3+UF_4$ was given by $p^*(N_2)=39.57-46\,950/T$ for $T=1103$–1148 K. Combining this $p(N_2)$ with ΔG_f°(UN(s)) by Matsui and Ohse [10] and ΔG_f°(UF_4(s)) by Fuger et al. [48], ΔG_f°(UF_3(s)) is estimated to be -1239 kJ mol^{-1} at 1100 K, which appears less negative by ~20 kJ mol^{-1} compared with the assessed values up to 800 K [46]. Also this $p(N_2)$ appears too high by a factor of two compared with the equilibrium $p(N_2)$ over $UN+U_2N_3$ [11].

A provisional stability diagram of the U–N–F system has been constructed (Fig. 7). Considering the apparent discrepancies with the literature data for UF_3 and U_2N_3, only the relative positions of phase regions are important.

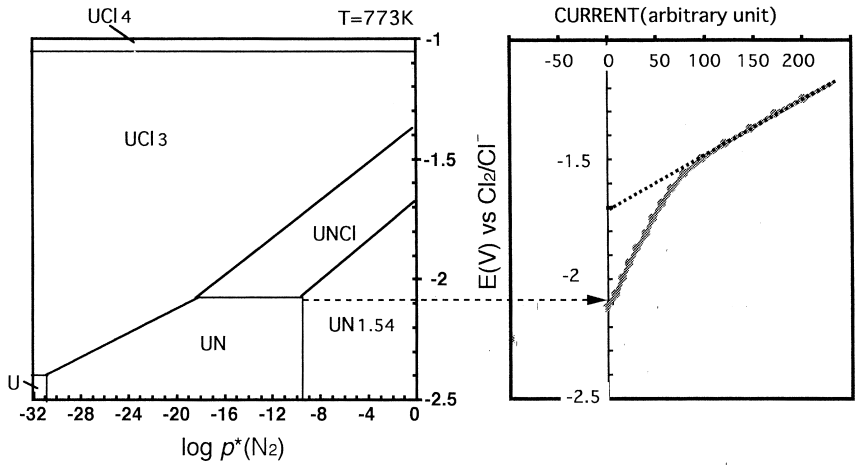

Fig. 6. Stability diagram of U–N–Cl system at 773 K (left), compared with the anodic decomposition curve of a UN pellet in a LiCl–KCl eutectic melt [46] (right).

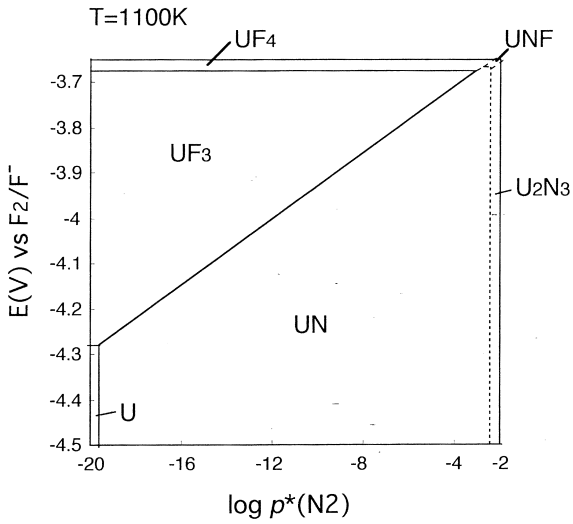

Fig. 7. Provisional stability diagram of U–N–F system at 1100 K.

The stability range of UNF in the top-right corner of the figure should extend up to $p^*(N_2)=1$.

3.3. Pu–N–Cl

There does not seem to be a ternary compound, at least for temperatures above the melting point of Pu (913 K) and $p^*(N_2)\leq 1$. Campbell [49] has obtained the e.m.f. of the cell, Pu(s, l)|$PuCl_3$, LiCl–KCl|N_2(g) (1 atm), PuN, by a galvanostatic potential determination. The ΔG_f°(PuN(s)) calculated from the e.m.f. values agrees with that in the literature at temperatures above the melting point of Pu. In view of the stability diagram of the U–N–Cl system in Fig. 6, this fact suggests that PuNCl is not a stable compound at nitrogen partial pressures to $p^*(N_2)=1$ in the Pu–N–Cl system at these high temperatures.

The free energy of formation of $PuCl_3$(s) is more negative than that of UCl_3(s) by about 90 kJ mol^{-1} at 773 K, giving the difference in e.m.f. of about -0.3 V. Besides, the enthalpy of formation of PuNCl should be less negative than UNCl, since the formal charge of metal ions in the nitride chloride is considered $4+$ from structural consideration [50] and the ionization energy (I_4) of plutonium is higher than that of uranium by 2 eV [51]. These factors nearly preclude the existence of PuNCl in the stability diagram of Pu–N–Cl at high temperatures.

References

[1] K. Nakajima, Y. Arai, Y. Suzuki, J. Nucl. Mater. 247 (1997) 33.
[2] T. Ogawa, T. Ohmichi, A. Maeda, Y. Arai, Y. Suzuki, J. Alloys Comp. 224 (1995) 55.
[3] F. Kobayashi, T. Ogawa, Y. Okamoto, M. Akabori, J. Alloys Comp. (this issue) 374–377.
[4] T. Ogawa, S. Yamagishi, F. Kobayashi, A. Itoh, T. Mukaiyama, M. Handa, R.G. Haire, Proc. Intern. Conf. on Evaluation of Emerging Nuclear Fuel Cycle Systems, Global 1995, 11–14 Sep., 1995, Vol. 1, Versaille, France, 1995, pp. 207–214.
[5] B. Sundman, J. Agren, J. Phys. Chem. Solids 42 (1981) 297.
[6] T. Ogawa, Scripta Metal. 16 (1982) 781.
[7] T. Ogawa, J. Nucl. Mater. 201 (1993) 284.
[8] O. Redlich, A.T. Kister, Ind. Eng. Chem. 40 (1948) 345.
[9] T. Matsui, R. Ohse, High Temp.–High Pres. 19 (1987) 1.
[10] G. Eriksson, K. Hack, Metall. Trans. B 21 (1990) 1013.
[11] H. Tagawa, J. Nucl. Mater. 51 (1974) 78.
[12] P.E. Potter, K.E. Spear, in: Thermodynamics of Nuclear Materials, IAEA, Vienna, 1979, pp. 195–227.
[13] F.L. Oetting, J.M. Leitnaker, J. Chem. Thermodyn. 4 (1972) 199.
[14] R. Benz, M.G. Bowman, J. Am. Chem. Soc. 88 (1966) 264.
[15] J. Bugl, A.A. Bauer, Joint US–Euratom Research and Development Report, Battel Memorial Institute, BMI-1692, 1964.
[16] W.M. Olson, R.N.R. Mulford, J. Phys. Chem. 67 (1963) 952.
[17] C.A. Alexander, J.S. Ogden, W.M. Pardue, J. Nucl. Mater. 31 (1969) 13.
[18] F.L. Oetting, M.H. Rand, R.J. Ackermann, The Chemical Thermodynamics of Actinide Elements and Compounds, Part 1: The Actinide Elements, IAEA, Vienna, 1976.
[19] T. Ogawa, J. Alloys Comp. 203 (1994) 221.
[20] C.B. Alcock, Atomic Energy Rev. 6 (1976) 28–31.
[21] Yu.F. Khromov, D.E. Svistonov, Izv. Akad. Nauka SSSR, Neorg. Mater. 27 (1991) 25.
[22] M.A. Eron'yan, R.G. Avarbe, T.A. Nikol'skaya, Izv. Akad. Nauka SSSR, Neorg. Mater. 12 (1976) 247.
[23] O. Kubaschewski von Goldbeck, Atomis Energy Rev. 6 (1976) 98–99.
[24] K.A. Gingerich, J. Chem. Phys. 51 (1969) 4433.
[25] Y. Ikeda, M. Tamaki, G. Matsumoto, J. Nucl. Mater. 59 (1976) 103.
[26] Yu.F. Khromov, D.E. Svistonov, Atomic Energy 49 (1980) 25.
[27] H. Inouye, J.M. Leitnaker, J. Am. Ceram. Soc. 51 (1968) 6.
[28] H. Tagawa, Nippon Genshiryoku Gakkaishi 12 (1970) 18–25.
[29] R.A. Kent, J.A. Leary, High Temp. Sci. 1 (1969) 176.
[30] C.A. Alexander, R.B. Clark, O.L. Kruger, J.L. Robins, in: H. Blank, R. Lindner (Eds.), Plutonium and other Actinides, North-Holland, Amsterdam, 1976, pp. 277–286.
[31] Y. Suzuki, A. Maeda, Y. Arai, T. Ohmichi, J. Nucl. Mater. 188 (1992) 239.
[32] W.M. Olson, R.N.R. Mulford, J. Phys. Chem. 68 (1964) 1048.
[33] J.P. Marcon, J. Poitreau, J. Inorg. Nucl. Chem. 32 (1970) 463.
[34] C.A. Alexander, J.S. Ogden, W.M. Pardue, Battelle Memorial Institute Report BMI-1872, Section A, pp. 1–3.
[35] C.A. Alexander, J.S. Ogden, W.M. Pardue, Battelle Memorial Institute Report BMI-1878, Section A, pp. 1–3.
[36] W.M. Olson, R.N.R. Mulford, J. Phys. Chem. 70 (1966) 2932–2934.
[37] R.J. Ackermann, E.G. Rauh, J. Chem. Thermodyn. 7 (1975) 211.
[38] Y. Arai, Y. Suzuki, M. Handa, Proc. Intern. Conf. on Evaluation of Emerging Nuclear Fuel Cycle Systems ''Global 1995'', 11-14 Sep., 1995, Vol. 1, Versaille, France, 1995, pp. 538–545.
[39] M.H. Bradbury, Hj. Matzke, Report European Institute for Transuranium Elements, EUR 5905, 1978.
[40] T. Ogawa, M. Akabori, F. Kobayashi, R.G. Haire, J. Nucl. Mater. 247 (1997) 215.
[41] R. Becker, H. Holleck, H. Kleikamp, L. Stieglitz, Gmelin Handbook of Inorganic Chemistry, Supplement Vol. C7, Springer, Berlin.
[42] Hj. Matzke, Science of Advanced LMFBR Fuels, North Holland, Amsterdam, 1986, pp. 67–89.
[43] R. Juza, W. Meyer, Z. Anorg. Allg. Chem. 366 (1969) 43.
[44] K. Yoshihara, M. Kanno, T. Mukaibo, J. Inorg. Nucl. Chem. 31 (1969) 985.
[45] I. Barin, Thermochemical Data of Pure Substances, 3rd ed., VCH Verlag, Weinheim, 1995.
[46] F. Kobayashi, T. Ogawa, M. Akabori, Y. Kato, J. Am. Ceram. Soc. 78 (1995) 2279.

[47] H. Tagawa, J. Inorg. Nucl. Chem. 37 (1975) 731.
[48] J. Fuger, V.B. Parker, W.N. Hubbard, F.L. Oetting, The Chemical Thermodynamics of Actinide Elements and Compounds, Part 8: The Actinide Halides, IAEA, Vienna, 1983.
[49] G.M. Campbell, J. Phys. Chem. 73 (1969) 350.
[50] K. Yoshihara, S. Yamaguchi, M. Kanno, T. Mukaibo, J. Inorg. Nucl. Chem. 33 (1971) 3323.
[51] L.R. Morss, in: J.J. Katz, G.T. Seaborg, L.R. Morss (Eds.), The Chemistry of the Actinide Elements, 2nd ed., Vol. 2, Chapman and Hall, New York, pp. 1278–1360.